

Peifang Tian¹, Ivan C. Teng¹, Anders M. Dale^{1,2} and Anna Devor^{1,2,3}

¹Departments of Neurosciences and ²Radiology, University of California, San Diego, CA, ³Martinos Center for Biomedical Imaging, MGH, Harvard Medical School, Charlestown, MA,

Introduction

A mechanistic understanding of the hemodynamic response requires a systematic analysis of single-vessel properties carried out in the framework of realistic vascular microarchitecture and with respect to the underlying neuronal activity. Previously, we used somatosensory stimulation and two-photon microscopy to study neurovascular coupling in rat primary somatosensory cortex [1]. Our results showed that on the level of single surface (pial) arterioles, the response was composed of dilatory and constrictive phases. Comparison of two-photon data with neuronal measurements demonstrated a correlation of the arteriolar constriction with enhanced neuronal inhibition. Here we extend the two-photon measurements across cortical depth and to the other two vascular compartments, capillaries and veins.

We measure changes in diameter and blood flow velocity of individual arterioles, capillaries and venules down to 500 μm in response to a somatosensory stimulus in rat primary somatosensory cortex (SI). We ask the following questions: (1) do penetrating arterioles and their branches show biphasic response similar to that of the pial arterioles? (2) does the arteriolar response depend on the cortical depth and local vascular geometry? (3) are there "hot spots" of arteriolar dilation consistent with anatomical literature [2-3]? (4) do veins/venules swell (dilate) in response to the stimulus? (5) is the velocity profile consistent with the diameter change?

[1] Devor A, et al., Suppressed neuronal activity and concurrent arteriolar vasoconstriction may explain negative blood oxygenation level-dependent signal. *J Neurosci* 27(16):4452-4459 (2007)
 [2] Rosen WC. The morphology of valves in cerebral arteries of the rat. *Anat. Rec* 157: 481-487 (1967)
 [3] Nakai K, et al., Microangiography of rat parietal cortex with special reference to vascular "sphincters". Scanning electron microscopic and dark field microscopic study. *Stroke* 12:653-659 (1981)

Methods

Rats were initially anesthetized with isoflurane (3% initially, 1-2% during ventilation) and ventilated with a mixture of air and oxygen during surgical procedures. During the surgery cannulas were inserted in the femoral artery and vein. Isoflurane was discontinued, and anesthesia was maintained with 50 mg \cdot kg⁻¹ intravenous bolus of α -chloralose followed by continuous intravenous infusion at 40 mg \cdot kg⁻¹ \cdot h⁻¹. Heart rate, blood pressure and body temperature were continuously monitored. Respiration was aimed to maintain pCO₂ between 35 and 45 mmHg.

An area of skull overlying SI was exposed, the skull and dura mater were removed, and the space between the exposed brain surface and the coverglass was filled with 0.7% (w/v) agarose (Sigma) in ACSF. To avoid herniation of the exposed brain due to excessive intracranial pressure, dura mater over the IVth cerebral ventricle was punctured and plastic PE50 tube was inserted to allow draining of cerebro-spinal fluid (CSF). The draining hole was sealed after sealing of the imaging well.

To visualize the vasculature, ~0.3 ml of 5% (w/v) solution of 2 MDa fluorescein-conjugated dextran (FD-200S, Sigma) in physiological saline was injected intravenously [4].

Images were obtained using Ultima 2-photon microscopy system from Prairie Technologies. We used a 4x air objective (Olympus XLFluor4x/340, NA=0.28) to obtain images of the surface vasculature across the entire cranial window to aid in navigating around the cortical vasculature. 20x (Olympus, NA=0.5) and 40x (Zeiss, NA=0.8) water-immersion objectives were used for high-resolution imaging and line scan measurements. Data analysis was performed in Matlab environment.

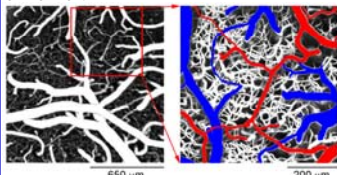


Figure 1. Two-photon image of the surface vasculature. The image on the left was calculated as a maximum intensity projection (MIP) of an image stack of 0-300 μm in depth. Individual images were acquired every 10 μm using 4x objective. The high-resolution image on the right was calculated as a MIP of a stack of 0-400 μm in depth. Individual images were acquired every 2 mm using 20x objective. Surface arterioles and venules are color-coded (red and blue, respectively).

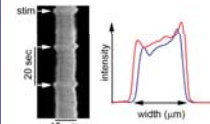


Figure 2. Measurements of vessel diameter from line-scan data. The diameter changes are captured by repeated line-scans across the vessel that form a space-time image when stacked sequentially (left). Diameters are extracted from profile changes (right: compare blue (baseline) to red (peak dilation)).

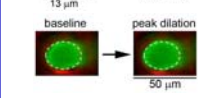


Figure 3. Measurements of vessel diameter from frame-scan data. Diameter can also be estimated from image time series of diving vessel obtained in a frame-scan mode by counting the number of pixels above a pre-set intensity threshold.

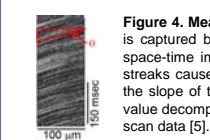


Figure 4. Measurements of velocity of red blood cells (RBCs). The velocity is captured by repeated line-scans along the axis of the vessel that form a space-time image when stacked sequentially and leads to the generation of streaks caused by the motion of RBCs. The speed is given by the inverse of the slope of these streaks (velocity=1/tan(θ)). An algorithm based on singular value decomposition is used to automate the calculation of speed from the line-scan data [5].

[4] Nishimura N, et al., Penetrating arterioles are a bottleneck in the perfusion of neocortex. *Proc Natl Acad Sci USA*, 104(1), 365-370 (2007)
 [5] Kleinfeld, D., et al., Fluctuations and stimulus-induced changes in blood flow observed in individual capillaries in layers 2 through 4 of rat neocortex. *Proc Natl Acad Sci U S A*, 95(26) 15741-6 (1998)

Dilation propagates towards the cortical surface along the main trunks of diving arterioles

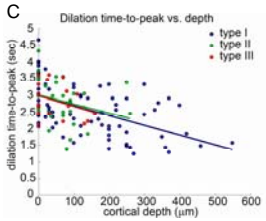
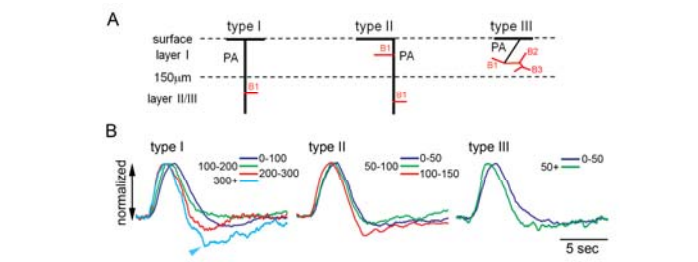


Figure 5. Arteriolar dilation and constriction along diving trunks of arteriolar trees before the 1st branching point. **A**, Schematic representation of three types of vascular geometry. **B**, Averaged response time-courses for each type. Responses from different depths are superimposed. Dilation is plotted upward; constriction – downward. For each type, depths are indicated in the inset. **C**, Time-to-peak of dilation as a function of the cortical depth. The three types of vascular geometry are superimposed in different colors.

For the same cortical depth, time-to-peak of the trunk precedes that of side branches

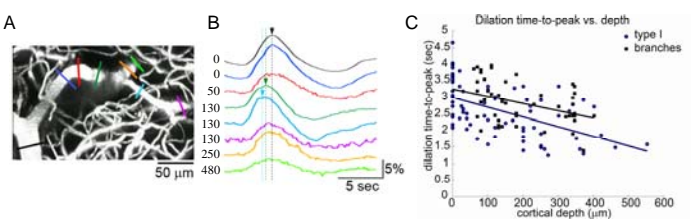


Figure 6. Dilation and constriction along branching arteriolar trees. **A**, The image, calculated as a MIP of an image stack of 0-300 μm , shows a branching diving arteriole. Individual images were acquired every 10 μm . **B**, Time-courses of arteriolar diameter changes along the branching tree. The locations of diameter measurements are color-coded in **A**. **C**, Time-to-peak of dilation as a function of the cortical depth. Branches (black squares) are superimposed on type I trunks (blue circles).

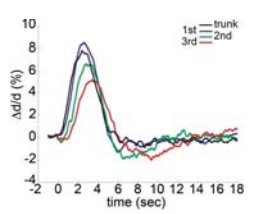


Figure 7. Dilation and constriction of arteriolar side branches and capillaries (baseline diameter of 5-13 μm), categorized by the branching order (blue, red and green), in comparison with diving trunks (black).

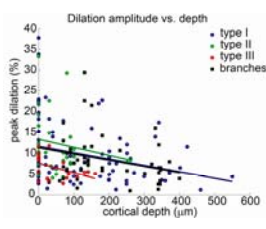


Figure 8. Peak amplitude of dilation as a function of the cortical depth. The three types of arteriolar trunks (blue, green and red) and side branches (black) are superimposed.

The relative constriction is a function of the distance from the center of neuronal response and the cortical depth

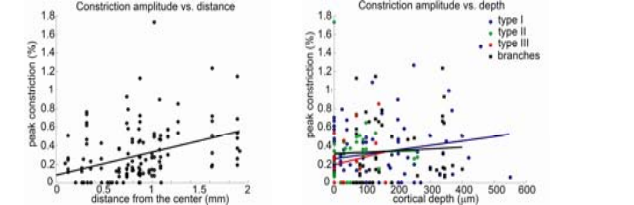


Figure 9. Relative peak amplitude of constriction as a function of the distance from the center (left) and as a function of the cortical depth (right). On the right, the three types of arteriolar trunks (blue, green and red) and side branches (black) are superimposed.

"Hot spots" are mainly located at branching points, both on the surface and throughout the measured cortical depth

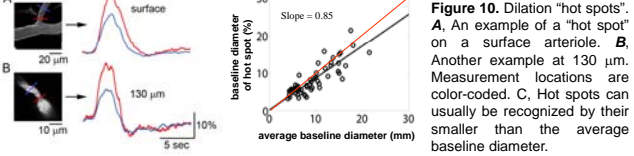


Figure 10. Dilation "hot spots". **A**, An example of a "hot spot" on a surface arteriole. **B**, Another example at 130 μm . Measurement locations are color-coded. **C**, Hot spots can usually be recognized by their smaller than the average baseline diameter.

RBCs velocity leads dilation

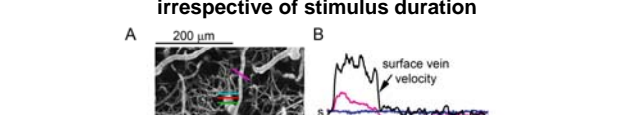


Figure 11. An increase in RBCs velocity (red) leads diameter changes (black) at all measured cortical depths. Averaged velocity and diameter response time-courses from the top 100 μm (solid lines) and 100-200 μm (dashed lines) are superimposed. These biphasic velocity time-courses indicate that RBCs flux is reduced during arteriolar constriction.

Veins do not dilate (swell) at any measured cortical depth irrespective of stimulus duration

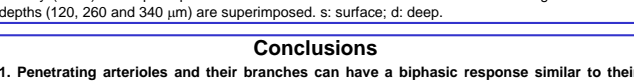


Figure 12. Veins do not dilate even during long stimulation. **A**, The image was calculated as a MIP of an image stack of 0-300 μm in depth. Individual images were acquired every 10 μm . **B**, Top: Time-courses of surface arteriolar (magenta) and venous (blue) diameter changes and venous velocity (black) are superimposed. Bottom: Time-courses of venous diameter changes at different depths (120, 260 and 340 μm) are superimposed. s: surface; d: deep.

- ### Conclusions
1. Penetrating arterioles and their branches can have a biphasic response similar to their parent surface arteries: the initial dilation followed by constriction. Relative to the initial dilation, a stronger constriction is observed (i) further away from the center of neuronal activity and (ii) deeper down the cortical tissue.
 2. Dilation propagates upstream towards the cortical surface along the main trunks of diving arterioles and invades side branches.
 3. The largest dilation is observed in the parent surface arterioles of types I and II (deep-diving).
 4. Dilation "hot spots" are mainly located near arteriolar branching points, both on the surface and throughout the measured depth. Most of them can be recognized by their bottleneck appearance.
 5. Veins do not swell but increase the flow velocity. Their velocity change is biphasic indicating that RBCs flux is reduced during arteriolar constriction.

Acknowledgements
 We gratefully acknowledge support from the NINDS (NS-051188 to AD and NIBIB (EB00790 to AMD)